

Free-standing graphene intercalated nanosheets on Si(111)

Trung T. Pham* and Robert Sporken**★

Abstract

By using electron beam evaporation under appropriate conditions, we obtained graphene intercalated sheets on Si(111) with an average crystallite size less than 11nm. The formation of such nanocrystalline graphene was found as a time-dependent function of carbon deposition at a substrate temperature of 1000°C. The structural and electronic properties as well as the surface morphology of such produced materials have been confirmed by reflection high energy electron diffraction, Auger electron spectroscopy, X-ray photoemission spectroscopy, Raman spectroscopy, scanning electron microscopy, atomic force microscopy and scanning tunneling microscopy.

Key words: Graphene on Si, porous graphene, graphitic carbon, Si substrate, 3D graphene, electron beamevaporation

* Dept. of Materials Technology, HCMC University of Technology and Education, Vietnam. And Nanotechnology Lab - SHTP Labs, R&D center

**Research Center in Physics of Matter and Radiation (PMR), University of Namur (FUNDP)

★ Corresponding author:

e-mail: trungpt@hcmute.edu.vn, tel: ++84-(0)903782080

※ Acknowledgment

Manuscript received Aug. 23, 2017; revised Sep. 18, 2017 ; accepted Sep. 19, 2017

This is an Open-Access article distributed under the terms of the Creative Commons Attribution Non-Commercial License

(<http://creativecommons.org/licenses/by-nc/3.0>) which permits unrestricted non-commercial use, distribution, and reproduction in any medium, provided the original work is properly cited.

I. Introduction

In recent years, graphene nanosheets have attracted much attention as an excellent material for the fabrication of power sources based on carbon compounds for various applications such as portable electronic devices, electric vehicles, and energy storage systems due to the high energy density, high operating voltage and low self-discharge rate. Known as the case of rechargeable lithium ion batteries (commercial Li-ion cells), graphite is commonly used as an anode electrode because of its high coulombic efficiency, acceptable specific capacity and cyclic performance by forming intercalation compounds from Li and C atoms as LiC_6 [1, 2]. However, theoretical specific capacity of the three dimensional graphite within the sp^2 carbon structure is quite low because of the limited Li-ion storage sites [3, 4]. Then, an alternative has recently been reported as graphene – the thinnest material made from a single layer of sp^2 bonded carbon atoms in a two-dimensional honeycomb crystal lattice, which possesses outstanding electrical, optical, thermal, and mechanical properties [4–9]. Therefore, enormous efforts during the past ten years have been devoted to grow, transfer and characterize graphene on various substrates using many different methods such as mechanical exfoliation of highly oriented

pyrolytic graphite (HOPG) [4], chemical vapor deposition (CVD) on metal substrates [10], electron beam evaporation [11–12], epitaxial growth on bulk SiC by thermal decomposition [13], etc. Although the aim is to produce large scale of graphene sheets for high-performance metal-oxide-semiconductor field-effect transistors (MOSFETs), graphene nanosheets become bigger advantages for energy storage due to their capacity in the same given volume of containers, which qualify as a potentially promising anode material for lithium ion batteries [14–15]. Therefore, finding a suitable method in order to produce a such nanosheets of graphene is highly desirable. However, production of such graphene nanosheets for that application is up to now only from using water suspension of graphene oxide (GO), followed by thermal reduction of deposited multilayers in order to obtain reduced-graphene oxide (rGO). Reduction of GO into graphene-like sheets results in a graphitic structure, but it still contains many defects [16, 17] which could impact more or less on the electrical conductivity of graphene. In addition, the uniform control of graphene nanosheets attached on the electrode plate for obtaining the optimal performance of device is also a challenge. To compete with this technique in the growth of a such nanocrystalline graphene for those potential applications, we developed a process to produce a free-standing graphene

intercalated nanosheets (3D porous-like structure) made of a few graphene layers on Si(111) by using an electron beam evaporation (EBE) in ultrahigh vacuum (UHV). EBE is considered as a potential method to produce super-clean and high quality of thin films on any arbitrary semiconductor substrates due to its *in-situ* deposition of atoms in UHV compared to other ones. From experimental evidences, it was found that the evolution of our porous graphene materials on Si(111) acts as a function of the growth time during carbon atoms deposition at a substrate temperature of 1000°C . The structural and electronic properties of our graphene nanosheets were examined in detail by reflection high energy electron diffraction (RHEED), Auger electron spectroscopy (AES), X-ray photoemission spectroscopy (XPS), Raman spectroscopy. In particular, we present here scanning electron microscopy (SEM), atomic force microscopy (AFM) and scanning tunneling microscopy (STM) images which establish unambiguously the graphitic nature of such materials.

II. Experimental details

Si(111) ($\rho > 50\ \Omega\cdot\text{cm}$, n-type) samples are obtained by annealing (up to 1000°C) in UHV (pressure below 2.0×10^{-10} mbar) until a nice 7×7 reconstruction is observed in RHEED and STM. Carbon is deposited using an e-beam

evaporator from Tectra GmbH with a graphite rod of 99.997% purity from Goodfellow Cambridge Ltd. Silicon is evaporated from resistively heated n-type silicon in the same chamber where carbon is deposited. The samples are prepared *in situ* by evaporating carbon on the Si(111) surface at a substrate temperature of 1000°C (measured with an IR pyrometer). The carbon deposition rate is measured by a quartz crystal oscillator. The pressure in the chamber is kept below 1.0×10^{-8} mbar during the evaporation. The experimental procedure for obtaining graphene nanosheets on Si(111) as described in Fig. 1.

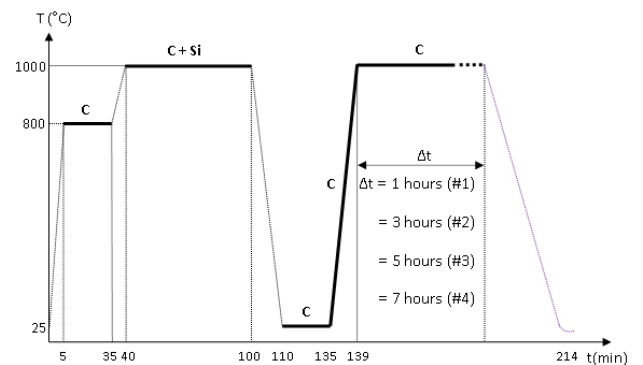


Fig. 1: A growth process for the formation of graphene nanosheets on Si(111) 7×7 substrate. Solid black line stands for C and Si flux ON.

First, the Si(111) surface is carbonized for 30 min at a substrate temperature of 800°C , followed by slowly heating to 1000°C (as detailed by Liu et al. [18] in order to obtain a good crystallinity of 3C-SiC film). After one hour for SiC formation at this temperature under carbon and silicon flux (the rate of Si and C is approximately $\sim 1.5:1$ in

which carbon evaporation rate is held constant at 7×10^{14} atoms. $\text{cm}^{-2} \cdot \text{min}^{-1}$), we stop the silicon and carbon flux and gradually decrease the substrate temperature to room temperature. Then, we restart carbon deposition on top of the sample for obtaining a few carbon layers (amorphous carbon) at this room temperature. After that, we slowly heat the sample (in about 4min) up to 1000°C during carbon deposition for various growth times as 1 hour (sample #1), 3 hours (sample #2), 5 hours (sample #3), 7 hours (sample #4). The carbon flux is then shut off and the sample is cooled down to 200°C at $20^\circ \text{C} \cdot \text{min}^{-1}$ and finally, free-cooled to room temperature.

Reflection high energy electron diffraction (RHEED, Riber), Auger Electron Spectroscopy (AES, Omicron) and STM (VP2 from Park Instrument) analyses were performed *in situ* while Raman, XPS and AFM were performed after transportation in the atmosphere. XPS analysis was made with a K-Alpha spectrometer from Thermo Scientific with a monochromated Al $K\alpha$ X-raysource (1486.6eV) and a resolution of 0.1eV. Raman scattering measurements were performed using a LabRamHR system with a 514nm laser excitation source and an objective of 100x. No outgassing was possible before performing the XPS, the Raman and the AFM measurements. The SiC and HOPG crystals used as references were analyzed in the same chambers after outgassing at 600°C for several hours (except

for the XPS and Raman measurements). An oxide layer is still present on the SiC after such outgassing [19] while the HOPG showed no oxygen contamination.

III. Results and discussion

Fig. 2 shows the RHEED patterns of the sample after SiC growth and followed by carbon layers deposition.

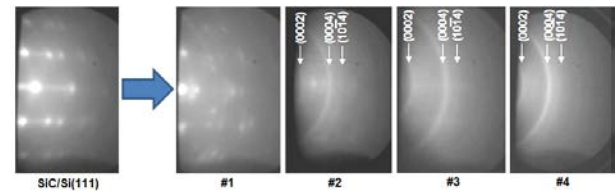


Fig. 2: RHEED patterns of the respective samples under various growth times on Si(1

As observed, the diffraction rings are visible in the RHEED patterns of the sample #1 after carbon deposition on top of SiC layers although they are still very faint. Besides SiC streaks, some Si faint spots could still be observed on the surface which is probably diffused from the substrate [20]. The rings appear more clearly in the samples #2, #3 together with very faint SiC streaks, meaning that carbide formation on the surface still occurs during this growth time and the SiC streaks disappear from RHEED patterns in the sample #4 after more carbon coverage. The sharp concentric rings are present for polycrystalline graphitic materials on top of the samples [12, 21] and position of these rings can

be determined as marked in the RHEED image in Fig. 2.

Based on this RHEED technique, the diffraction ring can be expressed by

$$\alpha = 2\theta_{\text{Bragg}} = \frac{R}{L}, \quad (1)$$

with θ_{Bragg} is very small, R is the ring radius and L is the distance from the sample to the phosphor screen. Combining (1) with the Bragg condition, the lattice spacing for hexagonal graphitic structure of a reciprocal lattice point with indices (hkl) will be found

$$d_{hkl} = \frac{\lambda L}{R}, \quad (2)$$

where L and λ are known, R is measured directly on the screen. By using the rings (0002) and (1014) in the sample #3, the lattice spacing in (2) is found to be $\sim 3.39 \text{ \AA}$ which is very close to the expected value for adjacent layers of graphite 3.35 \AA (error about 1.1%). Indeed, the derivatives of AES spectra around the CKLL transition on our samples were recorded in Fig. 3(a). Compared with the spectra of SiC and HOPG, it is clear that the shape of the curve of the sample #1 is similar to the one of SiC while the samples #2, #3, #4 are similar to the one of HOPG. The energy difference D between the maximum and the minimum of the curve was measured $\sim 22.6 \text{ eV}$ for samples #2 \rightarrow #4 as in HOPG and $\sim 11 \text{ eV}$ for sample #1 as in SiC.

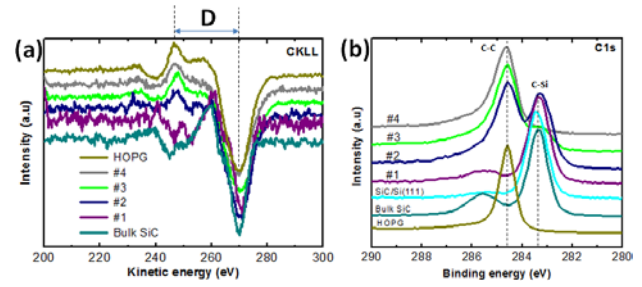


Fig. 3: (a) Differentiated AES spectra around the CKLL transition after carbon growth on top of the preformed SiC layers on Si(111) at 1000°C with different time of carbon deposition (samples #1 \rightarrow #4); (b) C 1s XPS spectra recorded on corresponding samples (HOPG and bulk SiC as references).

The graphitic properties of the carbon film on three samples #2, #3, #4 and the carbide on sample #1 are further confirmed by XPS data on C1s core level shown in Fig. 3(b). The spectrum shape of sample #1 is very similar to the SiC spectrum (except for the weaker component at 285.5 eV , which corresponds to the native oxide found on SiC[19]) while the others look similar with the one of HOPG. One can see that a transition from Si–C bonds to C–C bonds occurs gradually in those samples when the growth time is longer. The main peak of sample #2 appears at 284.7 eV (corresponding to C–C bonding) which is practically identical to the one of HOPG while a weaker component is still observed at 283.3 eV (corresponding to Si–C formation). This component is strongly reduced in sample #3 and disappeared in sample #4 with thicker graphitic carbon formation. It is consistent with the appearance of the faint SiC streaks in sample #2 and no longer observed in sample #4 as proposed by the RHEED patterns.

Raman measurements were performed using a

514 nm (2.41 eV) laser source to investigate the vibrations related to C–C bonds in the samples. The Raman spectra of four studied samples together with the commercial multi-wall carbon nanotubes (MWCNTs) and CVD single layer graphene (SL), included for comparison as plotted in Fig. 4 (a). The data reveals that the sample #1 does not show the typical sp^2 related signatures of C–C bonds in the systems while graphitic bonds are present on remaining samples in which the appearance of G (1587 cm^{-1}), 2D (2696 cm^{-1}) and defect-related D (1350 cm^{-1}) and D' (1620 cm^{-1}) bands confirm the graphitic nature of the grown layers, in good agreement with our AES and XPS characterization. In general, the presence of G and 2D bands is considered as characteristic for graphene [22]. Thus, it can be inferred that graphene layers formed on the surface of samples samples #2 \rightarrow #4.

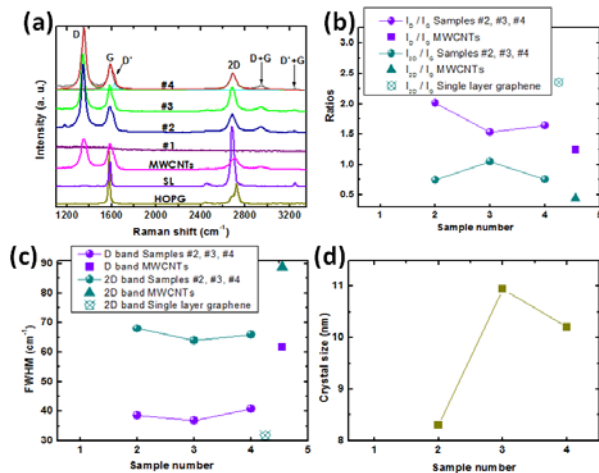


Fig. 4: (a) Raman measurements recorded at $\lambda = 514\text{ nm}$ ($E_{\text{laser}} = 2.41\text{ eV}$) of samples #1, #2, #3, #4, MWCNTs and CVD-produced single layer graphene; (b) corresponding intensity ratios; (c) FWHM of D and 2D bands and (d) crystal size of the measured samples derived from the I_D/I_G ratios.

Compared to HOPG, a few layers of graphene could be grown on our samples. According to our experimental process in Fig. 1, a thin SiC layer was produced before carbon deposition for graphene formation, which may induce a Raman shift of graphene related bands. Indeed, the G band of epitaxial graphene grown on C- and Si-terminated SiC has often similar frequency ($\sim 1586 - 1590\text{ cm}^{-1}$), which is upshifted from $\sim 6 - 10\text{ cm}^{-1}$ compared to that of HOPG ($\sim 1580\text{ cm}^{-1}$) [23, 24]. This is due to stress caused by the lattice mismatch between graphene and SiC. However, the 2D band is quite different in comparison with the one of HOPG (2726 cm^{-1}). For epitaxial multi-layer graphene on C-face SiC, it is $\sim 2730\text{ cm}^{-1}$ (higher) while it is 2702 cm^{-1} (lower) on Si-face SiC [25]. This is attributed to the interface interaction between graphene and Si-face SiC ($\sim 30\%$ of carbon atoms from the first graphene layer are covalently bonded to SiC [26, 27]), while such covalent bonds are absent at the interface between graphene and C-face SiC [13, 27]. The frequency of G and 2D bands of our materials is similar to that of epitaxial graphene on Si-face of 3C-SiC. A similar observation was made by Ouerghi et al. [28] who produced epitaxial graphene on Si-face 3C-SiC/Si(111) in UHV. However, the observation of these spectra reveals very intense defect-related bands (D and D' bands). By means of peak fittings (Lorentzian fittings for sample #4 as a representative), a quantitative analysis of the main spectral features was carried out and information about the intensities and FWHM (Full Width at Half

Maximum) of each peak were obtained. Fig. 4(b) summarizes the information about the intensity ratios I_D/I_G and I_{2D}/I_G of the graphitic samples and isolated points represent similar ratios calculated from MWCNTs and SL graphene data. The values for the I_{2D}/I_G ratios, ranging from 0.74 (sample #2), 0.75 (sample #4) to 1.05 (sample #3) indicate highly ordered structures, contrary to the low value of 0.44 for MWNTs (decrease in quality due to strong treatments for purification and functionalization). These high I_{2D}/I_G ratio values suggest that the crystalline areas might be constituted of two or more layers of graphene since the values of the FWHM of the 2D bands for these three samples lie around 60 cm^{-1} (see Fig. 4(c)), while the value for SL is $\sim 30\text{ cm}^{-1}$. Although these high intensities of the 2D band indicate the crystallinity of the samples, the values of the I_D/I_G ratios are even larger than the values of the I_{2D}/I_G ratios. Commonly, the presence of intense and broad D bands suggests defects in the honey-comb network, however, in this case the D bands are very sharp ($\sim 35 - 40\text{ cm}^{-1}$ in our samples contrary to $\sim 60\text{ cm}^{-1}$ for MWCNTs) which could be the indication of particular types of symmetry breaking elements like frontiers among polycrystals rather than vacancies or bare edges.

Also, further characterization is underway to determine the exact nature of these intriguing intense and sharp D bands. For the sake of relating the Raman data to crystal sizes, we have used the formula derived by Cancado et al.[29]. Results

indicate an average crystal size of 8–11 nm depending on the growth time as shown on Fig. 4(d).

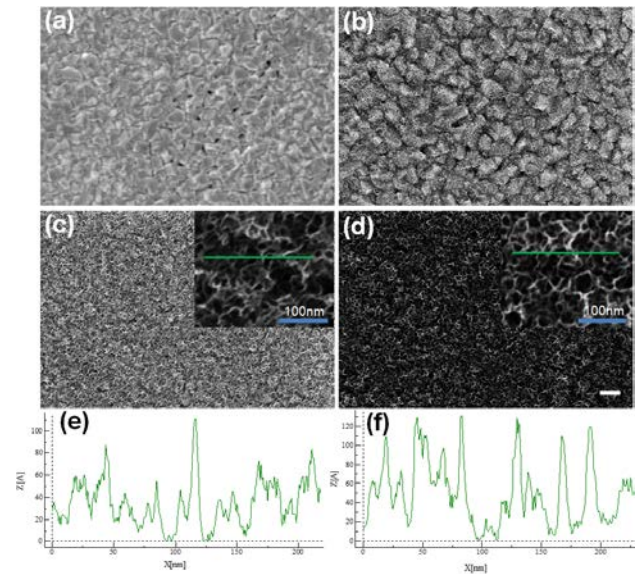


Fig. 5: SEM images taken from all studied samples showing the surface morphology of (a) sample #1, (b) sample #2, (c) sample #3, (d) sample #4. Scale bar is 200nm. (e) & (f) Height profiles measured from an inset in (c) and (d), respectively show the pore size as well as the wall height of our pores.

All studied samples are characterized by using SEM technique. Except for sample #1, it shows similar surface morphology with the formation of small porous-like structure as imaged on corresponding samples #2 → #4 for an illustration in Fig. 5. As observed, our materials are vertically aligned to the underlying substrate and are randomly intercalated to each other forming many small domains with dimensional size of 10 – 70 nm like a free-standing graphene intercalated nanosheets as proposed by Zhang et al.[30]. That is the reason why RHEED patterns suggest that these domains are randomly oriented (see above). In addition, the density

of nano-pores on the surface increases with an increase of the amount of deposited carbon atoms on the sample which is clearly visible in samples #2 \rightarrow #4. Also, the wall thickness of our porous graphene was measured about 1–2nm which equals to about 3–6 layers of graphene and the wall height of such material is estimated from 0 to 125Å depending on the area based on means of SEM profiling as taken on Figs. 5(e) & (f).

In order to confirm our above analyses, we took some STM and AFM images on the sample #3 (best sample) for more precise evaluation as shown in Fig. 6. A large-scale STM image of $2 \times 2 \mu\text{m}^2$ was performed with a root mean square roughness about 3.65 nm as presented in Fig. 6(a). The surface of our sample is quite rough with the formation of many domains which are made from tiny bunches of sp^2 bonded carbon nanosheets. This result is consistent with the observation of SEM images on this sample.

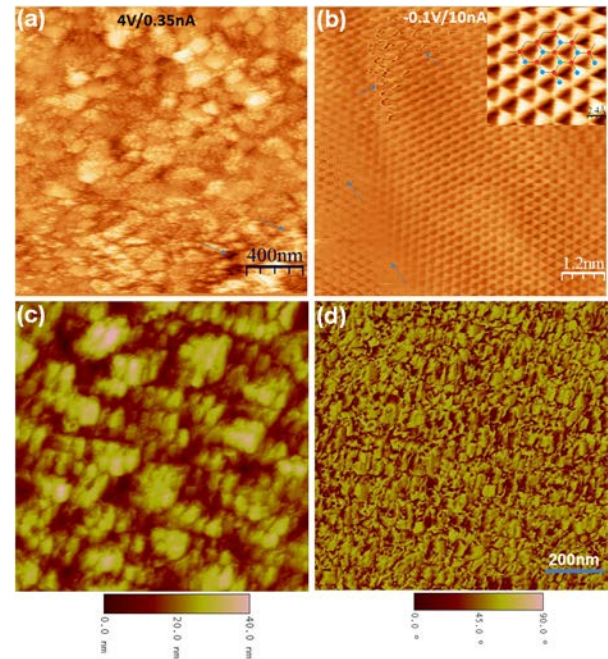


Fig. 6: (a) Large scale of STM image on sample #3: $2 \times 2 \mu\text{m}^2$ with tiny bunches which could be of graphene nanosheets and (b) a nano-scale image of $80 \times 80 \text{ \AA}^2$ with an inset of atomic resolution of the AB stacking in graphene layers with electronic noise marked by blue arrows. (c) Surface topographic AFM images of sample #3 and (d) the corresponding phase image.

Despite that roughness, the atomic resolution is still found at smaller scales of $80 \times 80 \text{ \AA}^2$ (Fig. 6(b)) together with an inset of $\sim 15 \times 15 \text{ \AA}^2$ taken on the same sample. Such an observation of triangular shape is in good agreement with STM measurements on HOPG which can be explained by the fact that the AB stacking of the layers in graphite breaks the symmetry, leading to two inequivalent carbon atoms per unit cell [31]. Therefore, they appear as the bright spots (blue dots) in the image where carbon atoms with a higher electron density lie directly above atoms in the plane below and represent only half the total number of carbon

atoms in the plane. Furthermore, Fig. 6(c) is an AFM surface topography image of sample #3, which shows a rather rough morphology containing many different grains and the corresponding AFM phase image obtained inside different graphene grains exhibits only weak contrast differences as seen in Fig. 6(d). It represents an indication that the differences in physico-chemical properties among the different grains are not large. In other words, our materials are homogeneous on this sample. This is in accordance with our XPS, Raman, SEM and STM analyses on this sample.

IV. Conclusions

In conclusion, we have grown free-standing graphene intercalated nanosheets as 3D porous graphene materials on Si(111) through the prior formation of several SiC layers, followed by a few layers of amorphous carbon deposited at room temperature which could act as a barrier to prevent out-diffusion of silicon atoms from the substrate during graphene formation at a substrate temperature of 1000° C. The experimental results confirmed a determinant influence of the growth time on the crystal evolution of graphene formation on Si(111). Especially, we obtained the real space SEM, AFM and STM images for an interpretation on the micro-/nano-structural properties of such 3D graphene materials.

V. Acknowledgments

Trung T. PHAM would like to thank Paul Thiry for useful discussions on RHEED patterns, Francesca Cecchet on AFM images and Etienne Gennart for technical support.

References

- [1] H. Nozaki, K. Nagaoka, K. Hoshi, N. Ohta, and M. Inagaki, "Carbon-coated graphite for anode of Lithium ion rechargeable batteries: Carbon coating conditions and precursors," *Journal of Power Sources*, vol. 194, no. 1, pp. 486 – 493, 2009.
- [2] L.-Z. Bai, D.-L. Zhao, T.-M. Zhang, W.-G. Xie, J.-M. Zhang, and Z.-M. Shen, "A comparative study of electrochemical performance of graphene sheets, expanded graphite and natural graphite as anode materials for Lithium-ion batteries," *Electrochimica Acta*, vol. 107, pp. 555 – 561, 2013.
- [3] J. Tarascon and M. Armand, "Issues and challenges facing rechargeable lithium batteries," *Nature*, vol. 414, no. 6861, pp. 197–200, 2001.
- [4] K. S. Novoselov, A. K. Geim, S. V. Morozov, D. Jiang, Y. Zhang, S. V. Dubonos, I. V. Grigorieva, and A. A. Firsov, "Electric field effect in atomically thin Carbon films," *Science*, vol. 306, pp. 666–669, 2004.
- [5] K. S. Novoselov, A. K. Geim, S. V. Morozov, D. Jiang, I. V. Katsnelson, I. V. Grigorieva,

- S. V. Dubonos, and A. A. Firsov, "Two-dimensional gas of massless dirac fermions in graphene," *Nature*, vol. 438, pp. 197–200, 2005.
- [6] A. K. Geim and K. S. Novoselov, "The rise of graphene," *Nature Materials*, vol. 6, pp. 183–191, Mar. 2007.
- [7] R. R. Nair, P. Blake, A. N. Grigorenko, K. Novoselov, T. J. Booth, T. Stauber, N. M. R. Peres, and A. K. Geim, "Fine structure constant defines visual transparency of graphene," *Science*, vol. 320, p. 1308, 2008.
- [8] A. A. Balandin, S. Ghosh, W. Bao, I. Calizo, D. Teweldebrhan, F. Miao, and C. N. Lau, "Superior thermal conductivity of single-layer graphene," *Nano Letters*, vol. 8, no. 3, pp. 902–907, Feb 2008.
- [9] C. Lee, X. Wei, J. W. Kysar, and J. Hone, "Measurement of elastic properties and intrinsic strength of monolayer graphene," *Science*, vol. 321, pp. 385–388, 2008.
- [10] J. Winterlin and M.-L. Bocquet, "Graphene on metal surfaces," *Surface Science*, vol. 603, no. 10–12, pp. 1841–1852, 2009.
- [11] P. Thanh Trung, F. Joucken, J. Campos-Delgado, J.-P. Raskin, B. Hackens, and R. Sporken, "Direct growth of graphitic carbon on Si(111)," *Applied Physics Letters*, vol. 102, no. 1, pp. 013118–n/a, 2013.
- [12] J. Tang, C. Y. Kang, L. M. Li, W. S. Yan, S. Q. Wai, and P. S. Xu, "Graphene films grown on Si substrate via direct deposition of solid-state carbon atoms," *Physica E*, vol. 43, no. 8, pp. 1415–1418, 2011.
- [13] J. Hass, W. A. de Heer, and E. H. Conrad, "The growth and morphology of epitaxial multilayer graphene," *Journal of Physics: Condensed Matter*, vol. 20, no. 32, pp. 323202–n/a, 2008.
- [14] X. Li, Y. Hu, J. Liu, A. Lushington, R. Li, and X. Sun, "Structurally tailored graphene nanosheets as Lithium ion battery anodes: an insight to yield exceptionally high Lithium storage performance," *Nanoscale*, vol. 5, pp. 12607–12615, 2013.
- [15] G. Kucinskis, G. Bajars, and J. Kleperis, "Graphene in Lithium ion battery cathode materials: A review," *Journal of Power Sources*, vol. 240, pp. 66–79, 2013.
- [16] S. Pei and H.-M. Cheng, "The reduction of graphene oxide," *Carbon*, vol. 50, no. 9, pp. 3210–3228, 2012.
- [17] F. Banhart, J. Kotakoski, and A. V. Krasheninnikov, "Structural defects in graphene," *ACS Nano*, vol. 5, no. 1, pp. 26–41, 2011.
- [18] Z. Liu, J. Liu, P. Ren, Y. Wu, and P. Xu, "Effects of carbonization and substrate temperature on the growth of 3C-SiC on Si by SSMBE," *Applied Surface Science*, vol. 254, no. 10, pp. 3207–3210, 2008.
- [19] L. Johansson, P.-A. Glans, and N. Hellgren, "A core level and valence band photoemission study of 6H-SiC(000-1)," *Surface Science*, vol. 405, no. 2–3, pp. 288–297, 1998.

- [20] T. T. Pham, C. N. Santos, F. Joucken, B. Hackens, J.-P. Raskin, and R. Sporken, "The role of SiC as a diffusion barrier in the formation of graphene on Si(111)," *Diamond and Related Materials*, vol. 66, pp. 141–148, 2016.
- [21] J. Hackley, D. Ali, J. DiPasquale, J. D. Demaree, and C. J. K. Richardson, "Graphitic carbon growth on Si(111) using solidsource molecular beam epitaxy," *Applied Physics Letters*, vol. 95, pp. 133114–n/a, 2009.
- [22] A. C. Ferrari, J. C. Meyer, V. Scardaci, C. Casiraghi, M. Lazzeri, F. Mauri, S. Piscanec, D. Jiang, K. S. Novoselov, S. Roth, and A. K. Geim, "Raman spectrum of graphene and graphene layers," *Phys. Rev. Lett.*, vol. 97, pp. 187401–n/a, Oct. 2006.
- [23] W. A. de Heer, C. Berger, M. Ruan, M. Sprinkle, X. Li, Y. Hu, B. Zhang, J. Hankinson, and E. Conrad, "Large area and structured epitaxial graphene produced by confinement controlled sublimation of silicon carbide," *Proceedings of the National Academy of Sciences*, vol. 108, no. 41, pp. 16900–16905, 2011.
- [24] N. Sharma, D. Oh, H. Abernathy, M. Liu, P. N. First, and T. M. Orlando, "Signatures of epitaxial graphene grown on Si-terminated 6H-SiC (0001)," *Surface Science*, vol. 604, no. 2, pp. 84–88, 2010.
- [25] O. Kazakova, V. Panchal, and T. L. Burnett, "Epitaxial graphene and graphene-based devices studied by electrical scanning probe microscopy," *Crystals*, vol. 3, no. 1, pp. 191–233, 2013.
- [26] J. D. Emery, B. Detlefs, H. J. Karmel, L. O. Nyakiti, D. K. Gaskill, M. C. Hersam, J. Zegenhagen, and M. J. Bedzyk, "Chemically resolved interface structure of epitaxial graphene on SiC(0001)," *Phys. Rev. Lett.*, vol. 111, pp. 215501–n/a, Nov. 2013.
- [27] K. V. Emtsev, F. Speck, T. Seyller, L. Ley, and J. D. Riley, "Interaction, growth, and ordering of epitaxial graphene on SiC(0001) surfaces: A comparative photoelectron spectroscopy study," *Phys. Rev. B*, vol. 77, pp. 155303–n/a, Apr. 2008.
- [28] A. Ouerghi, A. Kahouli, D. Lucot, M. Portail, L. Travers, J. Gierak, J. Penuelas, P. Jegou, A. Shukla, T. Chassagne, and M. Zielinski, "Epitaxial graphene on cubic SiC(111)/Si(111) substrate," *Applied Physics Letters*, vol. 96, no. 19, pp. 191910–n/a, 2010.
- [29] L. G. Cancado, K. Takai, T. Enoki, M. Endo, Y. A. Kim, H. Mizusaki, A. Jorio, L. N. Coelho, R. Magalhaes-Paniago, and M. A. Pimenta, "General equation for the determination of the crystallite size L_a of nanographite by Raman spectroscopy," *Applied Physics Letters*, vol. 88, no. 16, pp. 163106–n/a, 2006.
- [30] L. Zhang, F. Zhang, X. Yang, G. Long, Y. Wu, T. Zhang, K. Leng, Y. Huang, Y. Ma, A. Yu, and Y. Chen, "Porous 3D graphene-based bulk materials with exceptional high surface area and excellent conductivity for

supercapacitors," *ScientificReports*, vol. 3, no. 1408, 2013.

- [31] Y. Wang, Y. Ye, and K. Wu, "Simultaneous observation of the triangular and honeycomb structures on highly oriented pyrolytic graphite at room temperature: An STM study," *Surface Science*, vol. 600, no. 3, pp. 729–734, 2006.

BIOGRAPHY

Trung T. Pham (Member)



2002 : BS degree in Physical Electronics, University of Science Ho Chi Minh city, Vietnam.

2005 : MS degree in Physical Electronics, University of Science Ho Chi Minh city, Vietnam.

2015 : PhD degree in Physics and Nano Materials, University of Namur, Belgium.

2002~2015: Lecturer and researcher at Department of Physics, Faculty of Applied Sciences, HCMC University of Technology and Education, Vietnam.

2006~2007: Researcher at Nano Technology Laboratory, Saigon Hi-Tech Park, Vietnam.

2008~2009: researcher at Aeschlimann group of ultrafast phenomena at surfaces, Kaiserslautern, Germany.

2016~present: Senior researcher at Nano Technology Laboratory, Saigon Hi-Tech Park, Vietnam.

2016~present: Lecturer and researcher at Department of Materials Technology, Faculty of Applied Sciences, HCMC University of Technology and Education, Vietnam.

Robert Sporcken (Member)



1983: BS degree in Physics, Liège University, Belgium.

1983 : Agrégé de l'Enseignement Secondaire Supérieur, Liège University, Belgium.

1988 : PhD degree in Physics, University of Namur, Belgium.

1989–1991: Post-doctoral research associate, University of Illinois at Chicago, US.

1991–1993: Visiting professor, Université d'Aix–Marseille II (Marseille, France)

1992–2000: Senior researcher (chercheur qualifié), University of Namur, Belgium.

1997–present : Adjunct Professor, Department of Physics, University of Illinois at Chicago, US.

2000–2002: Associate Professor, University of Namur, Belgium.

2002–present: Professor University of Namur, Belgium.